Insights into conformational and packing features in a series of aryl substituted ethyl-6-methyl-4-phenyl-2-oxo-1,2,3,4-tetrahydropyrimidine-5-carboxylates†

Susanta K. Nayak,[a] K. N. Venugopala,[a] Deepak Chopra*[b] and T. N. Guru Row[a]

Received 29th March 2010, Accepted 10th August 2010
DOI: 10.1039/c0ce00045k

The supramolecular structures of eight aryl protected ethyl-6-methyl-4-phenyl-2-oxo-1,2,3,4-tetrahydropyrimidine-5-carboxylates have been analyzed to determine the role of different functional groups on the molecular geometry, conformational characteristics and the packing of these molecules in the crystal lattice. Out of these the *para* fluoro substituted compound on the aryl ring exhibits conformational polymorphism, due to the different conformation of the ester moiety. This behaviour has been characterized using both powder and single-crystal X-ray diffraction, optical microscopy and differential scanning calorimetry performed on both these polymorphs. The compounds pack *via* the cooperative interplay of strong N–H···O=C intermolecular dimers and chains forming a sheet like structure. In addition, weak C–H···O=C and C–H···π interactions impart additional stability to the crystal packing.

Introduction

In continuation of our efforts to understand the effect of functional groups on the conformational and packing features in the "Bignelli" class of compounds, we present here a systematic study of such features observed in these class of compounds containing the oxo moiety in place of the thioxo moiety.[1] These compounds contain multiple functional groups and exhibit significant conformational flexibility with respect to the aryl ring and the ester moiety. Both these functional groups can rotate independently with respect to the dihydropyrimidine (DHPM's) ring.[2,3]

For the relevant background literature, as regards application of these class of compounds, the reader is advised to refer to the previous article wherein we have performed similar studies on these class of compounds.[1] In view of tremendous application of these molecules, we have prepared a library of compounds where the ethyl-6-methyl-4-phenyl-2-oxo-1,2,3,4-tetrahydropyrimidine-5-carboxylate core is constant, and have undertaken to investigate the role of functional groups on molecular geometry, conformation and generation of supramolecular assemblies in the solid state. Furthermore, the synthesized compounds have also been evaluated for their antibacterial, *in vitro* antioxidant, and *in vitro* anti-inflammatory pharmacological activity by agar diffusion, and Bovine Serum Albumin method, respectively.[4]

Experimental

Synthesis

A mixture of ethylacetoacetate (0.1 mol), mono/di/tri substituted benzaldehyde (0.1 mol) and urea (0.1 mol) were refluxed in 50.0 mL of ethanol for 2.0 h in presence of concentrated hydrochloric acid as catalyst (Fig. 1). The reaction completion was monitored through thin layer chromatography and contents of the reaction mixture was poured into ice-cold water. The precipitate obtained was filtered, dried and crystallized from methanol to obtain the pure compounds. The purity of some of these samples were analyzed through melting point measurements (ESI, Table S1),†

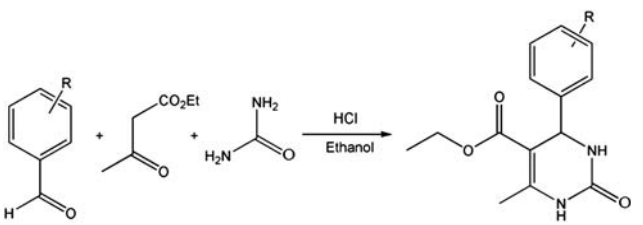

Fig. 1 Chemical scheme of the studied compounds: [**PYRO1**] R = *o*-F; 4-(2-fluoro-phenyl)-6-methyl-2-oxo-1,2,3,4-tetrahydro-pyrimidine-5-carboxylic acid ethyl ester. [**PYRO2**] R = *p*-F; 4-(4-fluoro-phenyl)-6-methyl-2-oxo-1,2,3,4-tetrahydro-pyrimidine-5-carboxylic acid ethyl ester. [**PYRO3**] R = *p*-Cl; 4-(4-chloro-phenyl)-6-methyl-2-oxo-1,2,3,4-tetrahydro-pyrimidine-5-carboxylic acid ethyl ester. [**PYRO4**] R = *p*-Br; 4-(4-bromophenyl)-6-methyl-2-oxo-1,2,3,4-tetrahydro-pyrimidine-5-carboxylic acid ethyl ester. [**PYRO5**] R = *p*-Me; 4-(4-methylphenyl)-6-methyl-2-oxo-1,2,3,4-tetrahydro-pyrimidine-5-carboxylic acid ethyl ester. [**PYRO6**] R = *p*-OMe; 4-(4-methoxyphenyl)-6-methyl-2-oxo-1,2,3,4-tetrahydro-pyrimidine-5-carboxylic acid ethyl ester. [**PYRO7**] R = *m*-OMe; 4-[3-methoxyphenyl]-6-methyl-2-oxo-1,2,3,4-tetrahydro-pyrimidine-5-carboxylic acid ethyl ester. [**PYRO8**] R = *m*-OMe, *p*-OH; 4-(3-methoxy-4-hydroxy-phenyl)-6-methyl-2-oxo-1,2,3,4- tetrahydropyrimidine-5-carboxylate acid ethyl ester.

[a]*Solid State and Structural Chemistry Unit, Indian Institute of Science, Bangalore, 560012, INDIA*
[b]*Indian Institute of Science Education and Research, ITI (Gas Rahat Building), Govindpura, Bhopal, 462023, INDIA. E-mail: dchopra@iiserbhopal.ac.in; Fax: +0755-4092392; Tel: +0755-4092321*

† Electronic supplementary information (ESI) available: Melting points, yields, IR data, PXRD and simulated Powder X-ray data. CCDC reference numbers 761378–761386. For ESI and crystallographic data in CIF or other electronic format see DOI: 10.1039/c0ce00045k

Table 1 Relevant crystallographic data

Data	PYRO1 (-*o*-F)	PYRO2a (-*p*-F)	PYRO2b (-*p*-F)	PYRO3 (-*p*-Cl)	PYRO4 (-*p*-Br)	PYRO5 (-*p*-Me)	PYRO6 (-*p*-OMe)	PYRO7 (-*m*-OMe)	PYRO8 (-*m*-(OMe)-*p*-OH)
Formula	$C_{14}H_{15}FN_2O_3$	$C_{14}H_{15}FN_2O_3$	C_{14} $H_{15}FN_2O_3$	$C_{14}H_{15}ClN_2O_3$	$C_{15}H_{15}BrN_2O_3$	$C_{15}H_{18}N_2O_3$	$C_{15}H_{18}N_2O_4$	$C_{15}H_{18}N_2O_4$	$C_{15}H_{18}N_2O_5$
CCDC number	761378	761379	761380	761381	761382	761383	761384	761385	761386
Formula weight	277.27	278.28	278.28	294.73	339.18	274.31	290.31	290.31	306.31
Colour	Colourless	Colourless	Colourless	Colourless	Colourless	Colourless	Colourless	Colourless	Colourless
Crystal morphology	Block	Plates	Rod	Block	Block	Cylindrical	Cylindrical	Prism	Plates
Crystal Size/mm	0.32 × 0.28 × 0.23	0.34 × 0.28 × 0.20	0.21 × 0.21 × 0.11	0.27 × 0.21 × 0.16	0.26 × 0.23 × 0.18	0.38 × 0.29 × 0.18	0.31 × 0.28 × 0.14	0.21 × 0.18 × 0.10	0.30 × 0.24 × 0.18
***T*/K**	292	120	120	120	292	120	120	292	292
Radiation	Mo-Kα	Mo-Kα	Mo-Kα	Mo-Kα	Mo-Kα	Mo-Kα	Mo-Kα	Mo-Kα	Mo-Kα
***λ*/Å**	0.71073	0.71073	0.71073	0.71073	0.71073	0.71073	0.71073	0.71073	0.71073
Crystal system	Triclinic	Monoclinic	Monoclinic	Monoclinic	Triclinic	Monoclinic	Monoclinic	Monoclinic	Monoclinic
Space group	$P\bar{1}$	$C2/c$	$P2_1/n$	$P2_1/n$	$P\bar{1}$	$P2_1/n$	$P2_1/n$	$P2_1/n$	$P2_1/n$
***a*/Å**	7.5291(6)	15.829(4)	12.0087(7)	12.7632(3)	7.5081(6)	12.7835(6)	15.7414(10)	12.2450(4)	12.2806(10)
***b*/Å**	9.0289(7)	7.2551(12)	7.3445(4)	7.3290(2)	8.6307(8)	7.3412(3)	7.3100(4)	7.4478(2)	7.4567(6)
***c*/Å**	11.2318(9)	24.285(4)	29.8816(15)	29.7055(10)	12.7259(11)	29.5499(14)	26.3147(14)	16.1914(5)	17.2659(14)
***α*/°**	106.417(1)	90	90	90	105.102(8)	90	90	90.0	90
***β*/°**	104.611(1)	106.972(5)	92.941(4)	93.705(2)	104.686(7)	93.462(4)	103.377(6)	106.676(3)	109.584(9)
***γ*/°**	100.197(1)	90	90	90	100.544(7)	90	90	90.0	90
***V*/Å^3**	682.88(9)	2667.4(9)	2632.0(2)	2772.88(14)	742.26(12)	2768.1(2)	2495.9(3)	1414.53(8)	1489.6(2)
Z	2	8	8	8	2	8	8	4	4
***D*/g mL^{-1}**	1.348	1.386	1.405	1.412	1.518	1.316	1.309	1.363	1.366
***μ*/mm^{-1}**	0.105	0.108	0.109	0.284	2.777	0.093	0.096	0.100	0.103
***F*(000)**	290	1168	1168	1232	344	1168	1232	616	648
***θ* (min, max)**	2.00, 24.99	3.11, 26.00	3.09, 29.36	3.26, 25.00	3.31, 25.99	3.10, 26.00	3.09, 26.00	3.00, 26.00	3.25, 26.00
Total no. of reflections	6549	18 255	30 240	25 976	15 967	28 107	30 736	14 691	15 352
No. of unique reflections	2399	2619	6454	4884	2908	5424	5768	2774	2923
No. of parameters	194	241	374	365	183	367	385	193	212
Treatment of hydrogens	Fixed	Refined all	Fixed	Fixed	Fixed	Fixed	Fixed	Fixed	Fixed
R_{obs}, w$R2_{obs}$	0.0537, 0.1313	0.0571, 0.1378	0.0568, 0.0958	0.0403, 0.1002	0.0615, 0.1467	0.0580, 0.1323	0.0504, 0.1186	0.0452, 0.1069	0.0525, 0.1437
$\Delta\rho_{min}$, $\Delta\rho_{max}$/e Å^{-3}	−0.273, 0.346	−0.266, 0.286	−0.286, 0.273	−0.393, 0.377	−0.433, 0.570	−0.264, 0.314	−0.274, 0.320	−0.223, 0.201	−0.250, 0.441
GOF	1.062	1.080	0.809	1.037	0.872	0.951	0.931	0.968	1.077

Table 2 Relevant experimental torsion angles (°)

Torsion	PYRO1	PYRO2A	PYRO2B (Molecule A/B)	PYRO3(Molecule A/B)	PYRO4	PYRO5 (Molecule A/B) PYRO6 (Molecule A/B)
C9–C4–C3–C5	68.1(2)	95.1(2)	86.4(4), 86.1(4)	84.5(2),88.7(2)	70.0(5)	85.0(3), 88.6(3) 83.5(2), 87.1(2)
C4–C3–C5–O2	−167.3(2)	−168.6(2)	−171.2(4), −175.0(3)	−171.8(2),−178.6(2)	−167.4(5)	−171.9(2), −172.4(2) −173.6(2), −170.1(2)
C9–C4–N2–C1	−99.9(2)	78.9(2)	85.7(3), 84.2(3)	87.6(2), 81.9(2)	99.5(5)	86.6(2), 81.1(2) 84.1(2), 85.5(2)
C14–C9–C4–C3	**52.7(2)**	**−30.1(3)**	**−27.1(3), −25.1(3)**	**155.8(2), 155.3(2)**	**38.4(6)**	**−31.5(3), −23.7(3) −9.7(3), 88.7(3)**
C4–N2–C1–N1	18.3(3)	19.9(3)	19.3(4), 20.8(4)	19.2(2), 22.6(2)	17.2(6)	20.3(3), 23.2(3) 24.4(3), 15.5(3)
C5–O3–C6–C7[a]	174.6(2)	86.8(3)	84.7(5), −176.3(3)	−78.9(2), 169.1(2)	105.8(5)	−77.9(3), 168.2(3) 164.2(2), −84.9(3)

Torsion	PYRO7	PYRO8
C9–C4–C3–C5	84.1(2)	85.4(3)
C4–C3–C5–O2	−171.4(2)	−166.5(3)
C9–C4–N2–C1	88.3(2)	83.7(2)
C14–C9–C4–C3	**6.5(2)**	**−173.7(2)**
C4–N2–C1–N1	15.6(2)	18.2(3)
C5–O3–C6–C7[a]	−177.5(2)	−169.2(4)

[a] In cases where the ethyl group (or one of the carbon atom) of the ester moiety is disordered, the torsion angle with respect to the major conformer is taken.

infrared spectroscopic data, ^{1}H-NMR, LC-MS. Furthermore, powder X-ray (PXRD) data were collected and compared with the simulated powder data obtained from single crystal data (see ESI)† thereby proving that the single crystal is representative of the bulk compound.

Data collection, reduction and refinement

A single crystal of suitable size (for **PYRO1**) for single-crystal X-ray diffraction was selected and data were collected on a Bruker AXS SMART APEX CCD diffractometer.[5] The X-ray generator was operated at 50 kV and 35 mA using Mo-Kα radiation ($\lambda = 0.71073$ Å). Data were collected with ω scan width of 0.3° at 292 K. A total of 606 frames were collected in four different settings of φ (0°, 90°, 180°, 270°) keeping the sample to detector distance fixed at 6.03 cm and the 2θ value fixed at −25°. The data were reduced using SAINTPLUS and an empirical absorption correction was applied using the package SADABS.[5] The remaining crystals (**PYRO2A**, **PYRO2B**, **PYRO3/5/6** are collected at 120 K and **PYRO4/7/8** at 292 K) were recollected in CrysAlis CCD, Oxford Diffraction with X-ray generator 49.30 kV and 0.980 mA, using Mo-Kα radiation ($\lambda = 0.7107$ Å).[5] The cell refinement, the data reduction was done in CrysAlis RED.[6] The structures were solved by direct method using SHELXL97[7] present in the program suite WinGX (version 1.70.01).[8] The molecular diagrams were generated from ORTEP[9] and the packing diagrams were generated using Mercury.[10] Geometrical calculations were done using PARST95[11] and PLATON.[12] The non-hydrogen atoms are refined anisotropically and hydrogen atoms bonded to C and N atoms were positioned geometrically and refined using a riding model with distance restraints of N–H = 0.86 Å, aromatic C–H = 0.93 Å, methyl C–H = 0.96 Å and with U_{iso}(H) = 1.2U_{eq}(N,C) and 1.5 U_{eq}(N,C).

Results

The molecular and crystal structures of all the eight compounds (**PYRO1–8**) have been determined at room temperature. The solid state molecular geometry were optimized for all the compounds using the Gaussian03 program package,[13] using B3LYP conjunction with the 6-31G** basis sets. Structures were visualized in the software MERCURY.[10] It is noteworthy that all the relevant torsion angles obtained from experiment and theory are comparable with each other, except for C14–C9–C4–C3, its magnitude depicting the rotational twist of the phenyl ring with respect to the six-membered tetrahydropyrimidine ring.

Fig. 1 depicts the chemical scheme of all the compounds under investigation. Table 1 lists the relevant crystallographic data and relevant torsion angles affected by functional group substitution, obtained from experiment are listed in Table 2. Table 3 lists all the intra- and intermolecular interactions observed in all the crystal structures.

The relevant bond lengths and bond angles are given in the ESI, Table S2.† Table S3 list the Cremer and Pople parameters[14] for the 6-membered rings, Table S4 lists the dihedral angles between the aryl ring with the tetrahydropyrimidine and carboxylic acid moiety. Table S5 lists the deviation of the flag-pole atoms C4 and N1 from the least squares plane passing through N2, C1, C2, and C3.† The list of torsion angles obtained from theory at the B3LYP/6-31G** are listed in Table S6.†

Structure of PYRO1

The molecular and crystal structure of 4-(2-fluoro-phenyl)-6-methyl-2-oxo-1,2,3,4-tetrahydro-pyrimidine-5-carboxylic acid ethyl ester has been determined previously.[15] It was observed that the magnitude of the residual peak was +0.856 eÅ^{-3}, which is high for a light atom structure. Hence it was of interest to re-determine the structure of the compound [Fig. 2]. It was observed that the fluorine atom at the *ortho* position is disordered over two sites, the major occupancy refining to 0.842(4). The residual electron density value is now +0.34 e Å^{-3}, an acceptable value for a light atom structure. This feature is present in many related organic compounds containing fluorine in either the *ortho* or *meta* position.[16] This compound crystallizes in the triclinic space group $P\bar{1}$ with $Z = 2$ molecules in the unit cell [Fig. 2]. The

Table 3 List of intra- and intermolecular interactions; Cg is the center of gravity of the isolated double bond C2═C3; Cg1 is the center of gravity of the six-membered aryl ring C9/C14; Cg2 is the center of gravity of the six-membered aryl ring C9′/C14′

Compound	D–H···A	*d*(D–H)/Å	*d*(H···A)/Å	*d*(D···A)/Å	∠(D–H···A)/°	Symmetry code
PYRO1	N1–H1N···O1	0.86	2.31	3.102(1)	154	$x+1, y, z$
	N2–H2N···O1	0.86	2.50	3.334(1)	165	$-x+1, -y, -z$
	C11–H11···F1	0.93	2.53	3.366(4)	150	$2-x, 2-y, 1-z$
PYRO2A	N1–H1N ···O1	0.85(3)	2.05(3)	2.890(3)	176(3)	$-x+3/2, -y+1/2, -z+2$
	N2–H2N···O1	0.89(3)	1.94(3)	2.832(3)	174(2)	$-x+3/2, -y+1/2+1, -z+2$
	C14–H14···O2	0.96(3)	2.46(3)	3.229(3)	136(2)	$x+1/2, y+1/2, z$
	C7–H7C···Cg1	0.90(4)	2.92(4)	3.707(4)	139(3)	$-1/2+x, 1/2+y, z$
	C11–H11···Cg1	0.96(2)	2.89(2)	3.540(3)	126(2)	$1/2-x, -1/2+y, 1/2-z$
PYRO2B	N1–H1N···O1′	0.88	2.11	2.926(3)	154	$x-1, y-1, z$
	N2–H2N···O1′	0.88	2.07	2.900(3)	157	$x-1, y, z$
	N1′–H1N′···O1	0.88	2.06	2.907(3)	161	$x+1, y+1, z$
	N2′–H2N′···O1	0.88	2.10	2.900(3)	152	$x+1, y, z$
	C11′–H11′···Cg1	0.95	2.81	3.534(3)	134	$1+x, y, z$
	C14–H14···O1′	0.95	2.81	3.685(3)	154	$x-1, y, z$
	C14′–H14′···O1	0.95	2.67	3.556(3)	156	$x+1, y, z$
	C13′–H13′···Cg2	0.95	2.84	3.703(3)	152	$3/2-x, -1/2+y, 1/2-z$
	C10–H10···O2	0.95	2.51	3.217(3)	131	$-x, -y+1, -z$
PYRO3	N1–H1N···O1′	0.88	2.06	2.894(2)	159	$3/2-x, -3/2+y, 1/2-z$
	N2–H2N···O1′	0.88	2.10	2.937(2)	158	$3/2-x, -1/2+y, 1/2-z$
	N1′–H1N′···O1	0.88	2.16	2.925(2)	145	$3/2-x, +3/2+y, 1/2-z$
	N2′–H2N′···O1	0.88	2.04	2.884(2)	160	$3/2-x, 1/2+y, 1/2-z$
	C14–H14···O1′	0.95	2.82	3.691(2)	153	$-x+3/2, y-1/2, -z+1/2$
	C14′–H14′···O1	0.95	2.62	3.518(2)	159	$-x+3/2, y+1/2, -z+1/2$
	C10–H10···O2	0.95	2.40	3.164(3)	137	$2-x, -y, -z+1$
	C11′–H11′···Cg1	0.95	2.93	3.734(2)	143	$x+1, y, z$
PYRO4	N1–H1N···O1	0.86	1.96	2.819(6)	172	$1-x, 2-y, -z$
	N2–H2N ···O2	0.86	2.30	3.130(6)	163	$-1+x, y, z$
	C14–H14···Cg	0.93	2.87	3.302(6)	121	x, y, z
PYRO5	N1–H1N···O1′	0.88	2.11	2.935(2)	156	$x, y-1, z$
	N2–H2N···O1′	0.88	2.10	2.923(2)	155	x, y, z
	N1′–H1N′···O1	0.88	2.05	2.897(3)	161	$x, y+1, z$
	N2′–H2N′···O1	0.88	2.16	2.925(3)	145	x, y, z
	C10–H10···O2	0.95	2.42	3.217(3)	141	$1-x, -y, -z$
PYRO6	N1–H1N···O1′	0.88	1.98	2.841(2)	166	$x-1, y-1, z$
	N2–H2N···O1′	0.88	2.16	2.940(2)	147	$x-1, y, +z$
	N1′–H1N′···O1	0.88	2.09	2.948(2)	164	$x+1, y+1, z$
	N2′–H2N′···O1	0.88	1.99	2.863(2)	174	$x+1, y, z$
	C11′–H11′···O2′	0.95	2.58	3.185(3)	122	$-x+3/2, y-1/2, -z+1/2$
	C14–H14···O1′	0.95	2.54	3.456(2)	161	$x-1, y, z$
PYRO7	N1–H1N···O1	0.86	2.13	2.966(2)	164	$-1/2-x, 1/2+y, 1/2-z$
	N2–H2N ···O2	0.86	2.09	2.922(2)	162	$-1/2-x, -1/2+y, 1/2-z$
	C12–H12···O2	0.93	2.64	3.524(3)	160	$-x+3/2, y+1/2, -z+3/2$
	C7–H7C···Cg1	0.98	2.97	3.780(3)	143	$1/2+x, 1/2-y, 1/2+z$
PYRO8	N1–H1N···O1	0.86	2.16	3.015(2)	171	$-1/2-x, -1/2+y, 1/2-z$
	N2–H2N···O1	0.86	2.09	2.902(2)	156	$-1/2-x, 1/2+y, 1/2-z$
	O4–H4O···O2	**0.82**	**2.33**	**2.872(3)**	**124**	$\mathbf{-x+1/2, y+1/2, -z+1/2}$
	C7–H7A···Cg1	0.98	2.97	3.759(4)	140	$1/2+x, 1/2-y, 1/2+z$
	C11–H11···Cg1	0.98	2.97	3.735(3)	141	$1/2-x, -1/2+y, 1/2-z$

compound exists in the screw boat conformation with C4 and N1 forming the flagpole atoms. The carbonyl group C5═O2 exists in an *s-cis* conformation [The spatial arrangement of two conjugated double bonds about the intervening single bond is described as *s-cis* if *synperiplanar* and *s-trans* if *antiperiplanar*] with respect to the C2═C3 double bond. The six-membered tetrahydropyridimine ring exhibits a dihedral twist of 89.3(1)° with the aryl ring. There are two potential hydrogen bond donors, namely H1N and H2N and two potential acceptors, namely the carbonyl oxygen atom O1 and O2, respectively. The crystal packing is characterised by two unique distances, depicted as *d*1 and *d*2 [Fig. 3] which separates the polar sheets in the crystal packing (across the center of symmetry). The distance *d*1 is almost invariant in all the crystal structures analyzed here, whereas *d*2 depends on the size and nature of the functional group (whether it is involved in intermolecular interactions) present on the phenyl moiety (termed as "hydrophobic spacer"). The distance *d*1 and *d*2 between two consecutive sheets is ~3.342(3) Å and ~7.649(3) Å. The crystal packing consists of N–H···O hydrogen bonded dimers, involving H1N, and chains, involving H2N along the crystallographic *a*-axis. This results in the generation of a sheet-like structure, forming $R^4_4(20)$[17] dimeric motifs [Fig. 4(a)]. The fluorophenyl moiety which separates two successive sheets provides additional stability *via* the formation of C–H···F dimeric motifs in the crystal lattice.[18] Fig. 4(b) shows the packing diagram depicting such motifs in the crystalline lattice. Such packing motifs have been frequently encountered in previous studies performed on compounds containing organic fluorine.[19] The consecutive sheets are held by van der Waals interactions between the molecules.

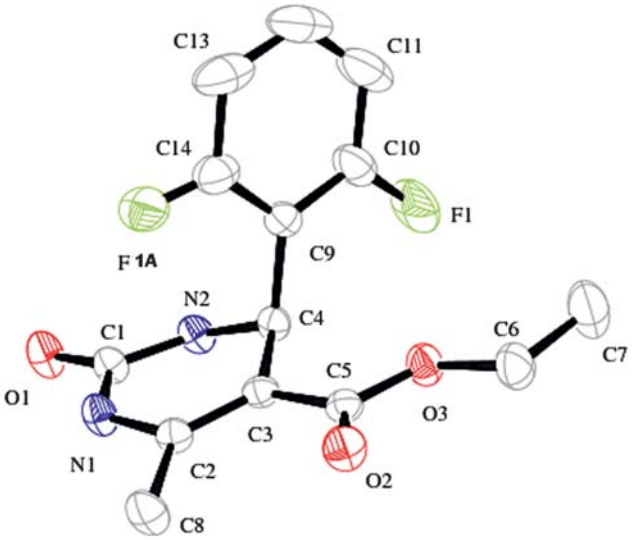

Fig. 2 ORTEP for **PYRO1** drawn at 50% ellipsoidal probability. The ester moiety exists in *s-cis* orientation with respect to the C2═C3 double bond. The hydrogen atoms have been excluded for clarity.

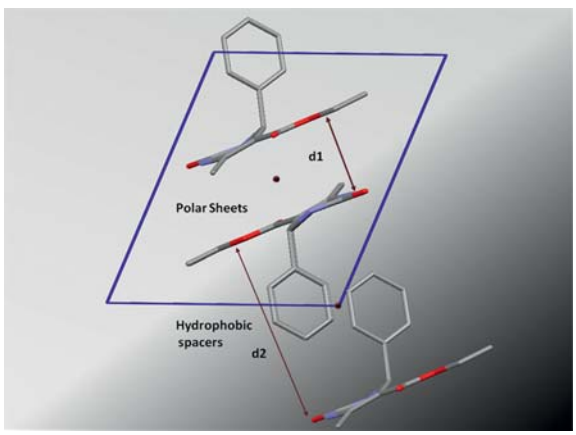

Fig. 3 Crystal packing in 6-methyl-4-phenyl-2-oxo-1,2,3,4-tetrahydropyrimidine-5-carboxylate ethyl ester, containing phenyl moiety. The blue line indicates the unit cell for a triclinic system (as reference for comparison). The coloured dots indicate the center of symmetry for the monoclinic crystal system.

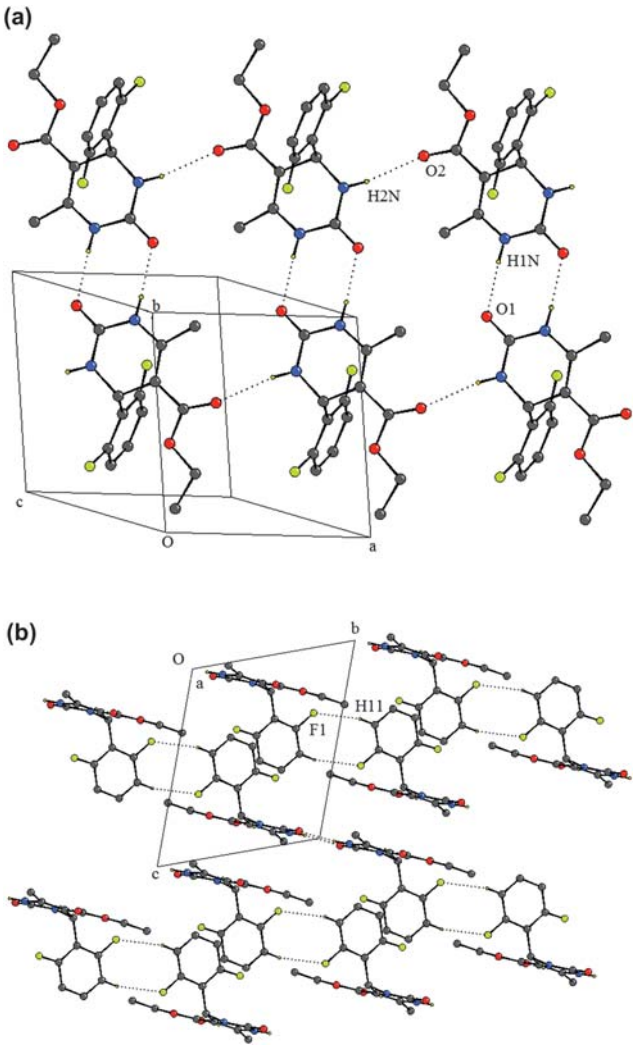

Fig. 4 (a): N–H···O hydrogen bonds generating a sheet-like structure. H atoms not involved in intermolecular interactions are omitted for clarity. (b): Packing diagram of **PYRO1** depicting N–H···O intermolecular hydrogen bonded dimers and chains along with C–H···F intermolecular interactions forming dimers. The N–H···O hydrogen bonds are perpendicular to the *bc* plane (along *a* axis).

Structure of PYRO2

The crystallization of this molecule results in the formation of concomitant dimorphs, exhibiting plate-like and rod shape morphology [Fig. 5]. Both forms crystallize in the monoclinic crystal system, having centrosymmetric space groups *C*2/*c* (**PYRO2A**: Form I) and $P2_1/n$ (**PYRO2B**: Form II), respectively. The number of molecules in the asymmetric unit is one [Fig. 6(a)] and two (Molecule A and B) [Fig. 6(b)] in the two forms. The ethyl group of the ester moiety is ordered in Form I and out of two molecules in the asymmetric unit, the ethyl group in one (Molecule A) is disordered in Form II. The occupancy for the major conformer (Molecule A) refines to a value of 0.640(6). Dihedral angles between the six-membered tetrahydropyrimidine ring and the aryl ring are 81.7(1)° in case of **PYRO2A** and 76.3(1)°/76.7(1)° in Molecule A/B for **PYRO2B**, respectively.

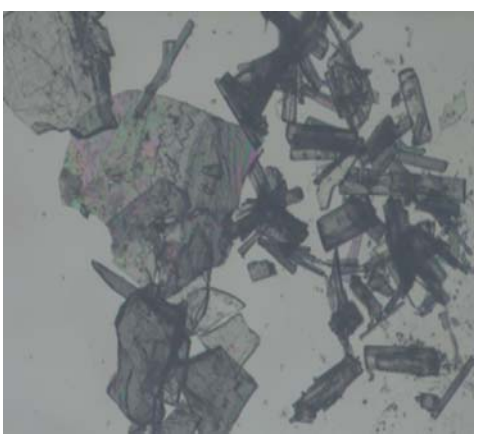

Fig. 5 Optical images depicting concomitant dimorph formation, existing in plate-like and rod shaped morphology.

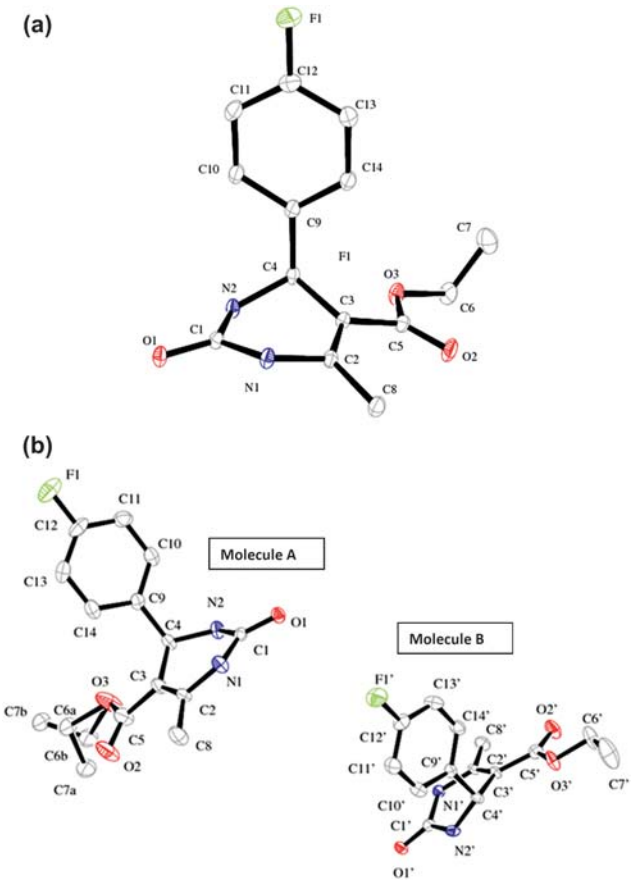

Fig. 6 (a) ORTEP for **PYRO2A** drawn at 50% ellipsoidal probability. The hydrogen atoms have been excluded for clarity. (b) ORTEP for **PYRO2B** depicting molecules A and B (asymmetric unit). The ester moiety exists in *s-cis* orientation with respect to the C2═C3 double bond. The hydrogen atoms have been excluded for clarity.

The orientation of the –OEt moiety is different in both the forms. In the former (Form I), the ethyl group is perpendicular to the carboxylate group, the torsion C5–O3–C6–C7 = 86.8(3)°, with respect to the ester moiety, the Molecule A, existing in two conformations, the conformation of the major conformer being similar with the one observed in Form I [torsion angle C5–O3–C6A–C7A = 84.7(5)°]. However, in Molecule B, the ethyl group and carboxylate moiety lie in the same plane, the torsion angle being −176.3(3)°. This leads to the formation of conformational dimorphs. The conformation of the ester moiety is *s-cis* with respect to the C2–C3 double bond in Molecule A and B, respectively. The existence of polymorphism in this compound is further supported by DSC experiments, the difference in the melting points of these dimorphic forms of **PYRO2** being 4.2 °C [Fig. 7].

The crystal packing in both the forms is formed *via* the involvement of strong hydrogen bonds and weak interactions. In Form I, in addition to N–H···O═C hydrogen bonds which form a sheet-like structure (ribbon motif), C–H···O═C (ester moiety) hydrogen bonds between the aromatic hydrogen (H14) of the aryl ring and the oxygen of the ester moiety provide additional stability. The space between the "polar" sheets is separated by a fluorophenyl spacer and is stabilized by C–H···π interactions[20] (involving H11). The adjacent sheets are held together by C–H···π intermolecular interactions (involving H7C) in the crystal packing [Fig. 8(a)]. The distances *d*1 and *d*2 are ∼3.823(3) Å and ∼9.094(5) Å, respectively. In both the forms, the primary packing motif consists of N–H···O dimeric hydrogen bonded ribbon motifs forming a sheet like structure along the *b* axis. In comparison to Form I, in Form II, there are two "unique" ribbon motifs, one in which a given Molecule A, is surrounded by Molecule B on either side to form ···BAB··· type of packing. In the other ribbon motif, a molecule B is surrounded by Molecule A on either side generating a ···ABA··· type of packing motif [Fig. 8(b)]. Overall, both the ribbon motifs are the same except that these are stacked one above the other, the distance between such successive layers being 3.494 Å. In addition, C–H···O intermolecular hydrogen bonds (involving H14), also provide additional stability. It is noteworthy, that C–H···π interactions exist between A and B molecules and also between molecules of the B-type which contribute towards the stability existing between the sheets [Fig. 8(c)]. The characteristic distances *d*1 and *d*2 are ∼3.315(3) Å and ∼8.490(4) Å (between molecule A and B in the unit cell). These are lower in magnitude compared to those observed in the previous form, thereby indicating higher packing efficiency (higher density of 1.405 in **PYRO2B** as compared to 1.386 in **PYRO2A**), accompanying a higher melting point for **PYRO2B** as observed in the thermal measurements.

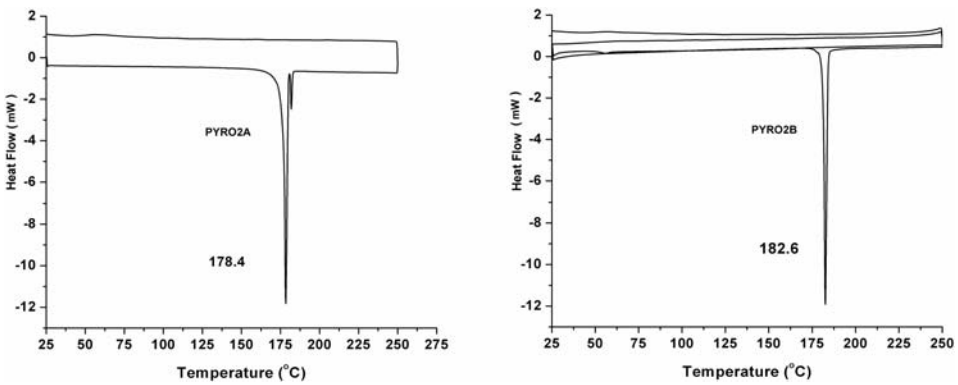

Fig. 7 DSC traces for the two dimorphs of **PYRO2**. The number of heating and cooling cycles were one for **PYRO2A** and two for **PYRO2B** (the rate of heating/cooling was 5 °C min^{-1}). In both forms, the absence of a crystallization exotherm indicates decomposition of the crystal after melting.

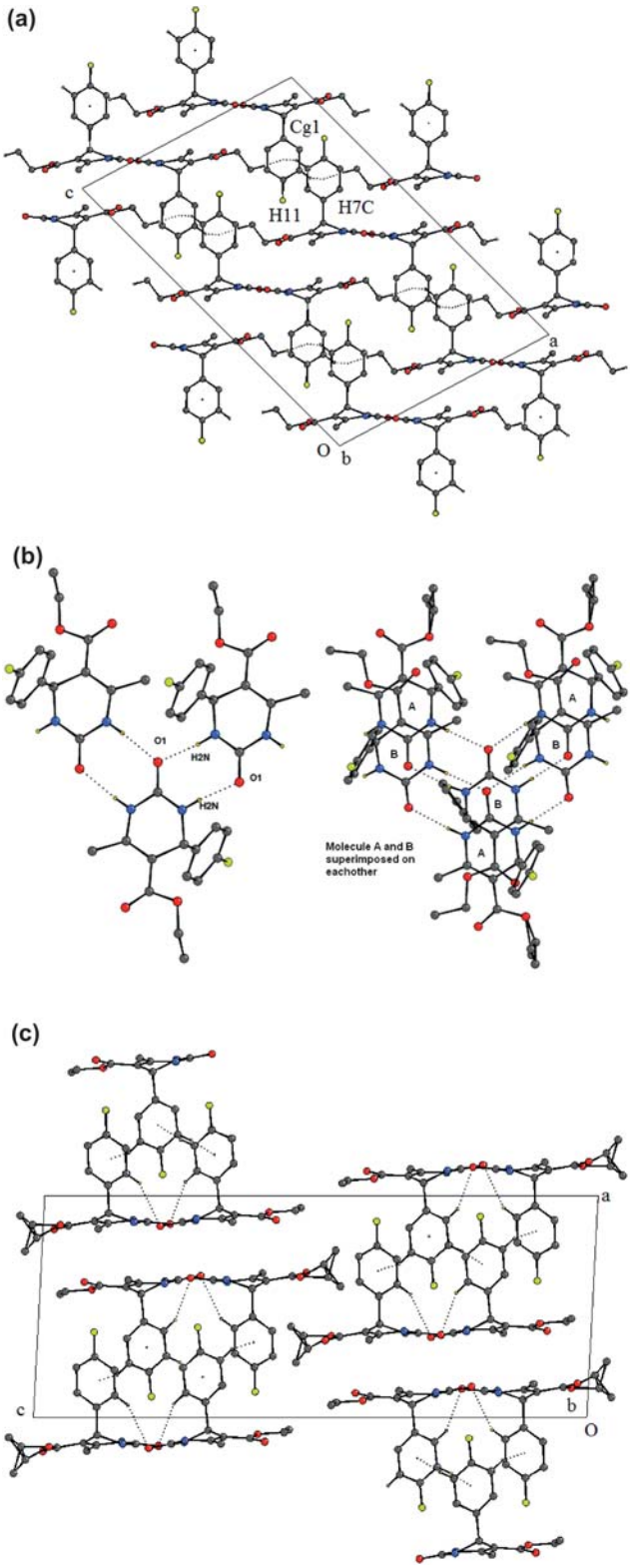

Fig. 8 (a) Packing diagram of **PYRO2A** depicting N–H···O═C hydrogen bond, C–H···O and C–H···π interactions. (b) **PYRO2A** forming ribbon motif whereas **PYRO2B** forming two superimposed ribbon motifs corresponding to "···ABA···" type of packing. (c) Packing diagram of **PYRO2B** depicting N–H···O═C hydrogen bonds, C–H···O and C–H···π interactions. H atoms not involved in intermolecular interactions are omitted for clarity.

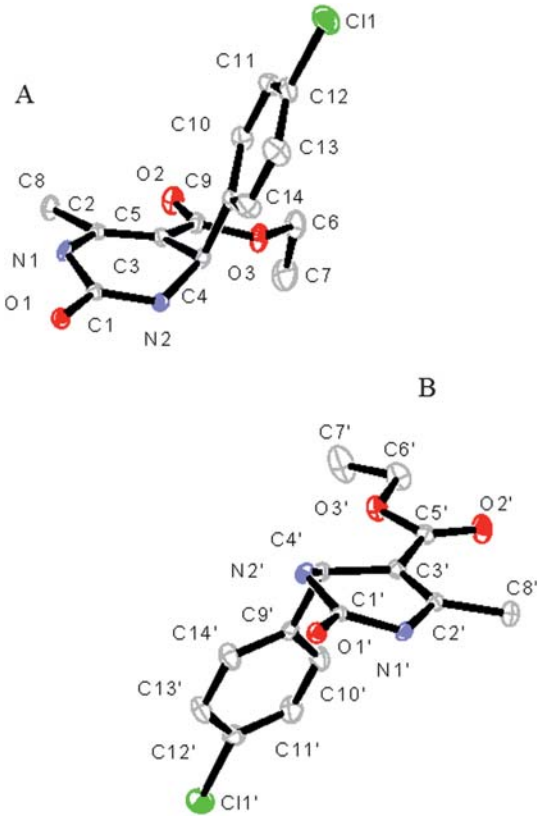

Fig. 9 ORTEP for **PYRO3** drawn at 50% ellipsoidal probability depicting molecules A and B (asymmetric unit). The ester moiety exists in *s-cis* orientation with respect to the C2═C3 double bond. The hydrogen atoms have been excluded for clarity.

Structure of PYRO3

The substitution of chlorine atom in the *para* position on the phenyl ring, results in the molecule crystallizing in the monoclinic space group $P2_1/n$ with $Z = 8$ ($Z' = 2$ [Fig. 9]) molecules in the unit cell.

The ester group exists in *s-cis* orientation with respect to the double bond. The aryl ring makes a dihedral twist of 73.8(1)°/79.8(1)° with respect to the tetrahydropyrimidine ring, for the two molecules respectively. N–H···O═C hydrogen bonded dimers involving all the highly acidic donors, namely H1N, H2N, H1N′ and H2N′ with the acceptor atoms O1 and O1′ form dimeric motifs leading to the formation of ribbons in the crystal structure along the crystallographic '*b*' axis. In addition C–H···O dimers further act cooperatively stabilizing the ribbon motifs [Fig. 10(a)]. The space between two successive sheets is stabilized by C–H···π intermolecular contact (involving H11′ and Cg2) due to the rotation along the C–C bond of the aryl ring [Fig. 10(b)]. There are no short contacts involving the chlorine atoms in the crystal lattice. The distance *d*1 and *d*2 between two successive sheets is ~3.338(3) Å and ~8.948(3) Å, respectively, (between molecule A and B in the unit cell). These distances and the nature of intermolecular contacts are comparable with those observed in **PYRO2B** indicating similarity in the crystal packing in the lattice.

Structure of PYRO4

The presence of the heavier halogen, bromine, in the *para* position on the phenyl ring results in the molecule crystallizing in the

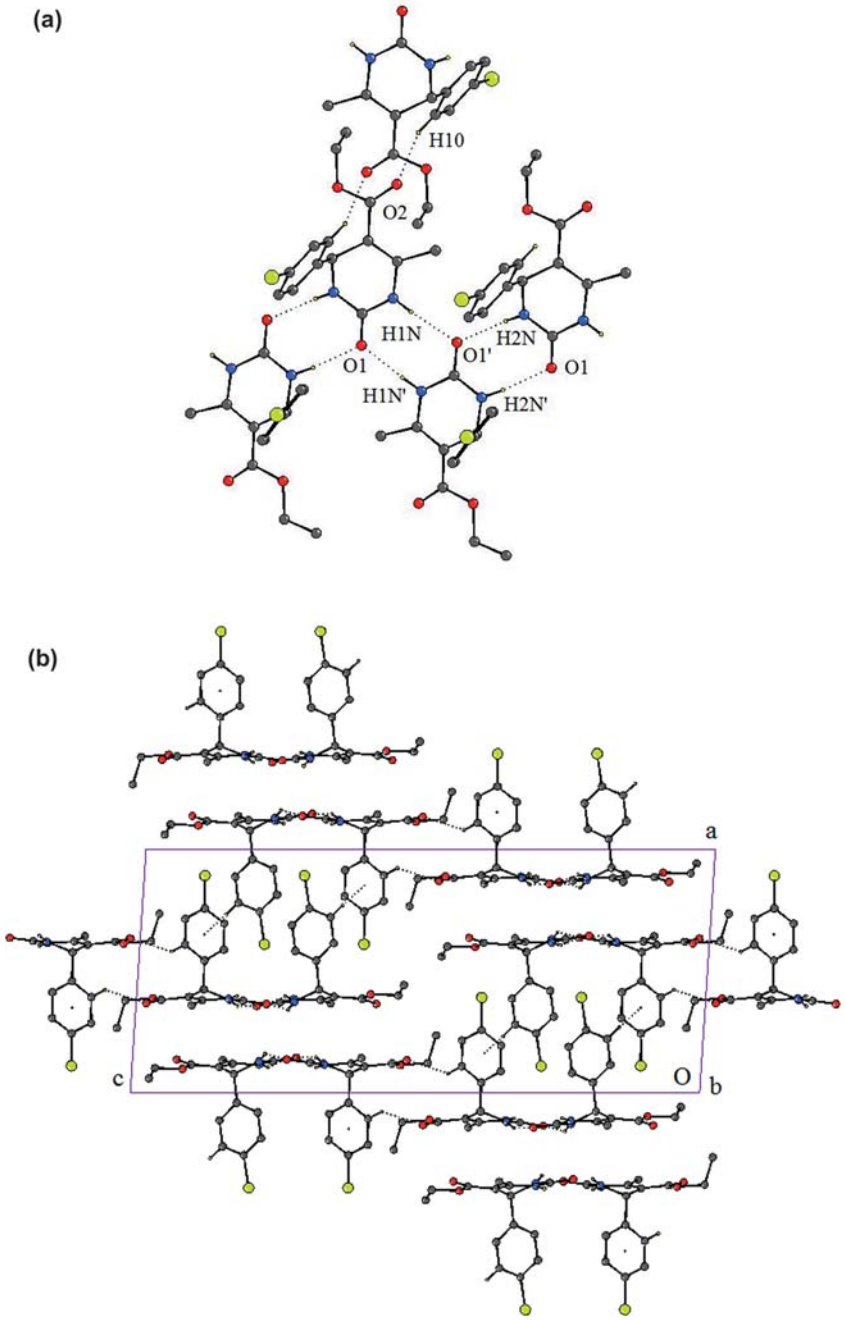

Fig. 10 (a) N–H···O hydrogen bonds depicting the formation of a ribbon motif stabilized by C–H···O interactions in **PYRO3**. (b) Packing diagram of **PYRO3** depicting N–H···O hydrogen bonds perpendicular to the *ac* plane along with C–H···π intermolecular contact between the sheets separated by the hydrophobic spacer. H atoms not involved in intermolecular interactions are omitted for clarity.

triclinic space group $P\bar{1}$ with $Z = 2$ molecules in the unit cell. The molecule exists in the screw boat conformation which is further locked by an intra-molecular C–H···π interaction [Fig. 11]. This feature has already been well investigated in the previously studied compounds containing thioxo moiety.[1] The ester group exists in *s-cis* orientation with respect to the double bond. The tetrahydropyrimidine and the aryl ring are nearly orthogonal to each other, the dihedral twist being 86.4(2)°. The carbon atom C7 is disordered over two sites, the major occupancy refining to a value of 0.57(1) and the minor being 0.43(1). The crystal packing is built up from interplay of hydrogen bonds involving strong donors and acceptors, namely H1N and H2N, forming N–H···O=C hydrogen bonds, generating a 2D-sheet like structure, forming a $R^4_4(20)$ ring motif [Fig. 12(a)]. The crystal structure is stabilized by additional short Br1···O1=C1 contacts [3.240 Å, 166°; symmetry code: $1 - x$, $2 - y$, $1 - z$] between the sheets separated by the hydrophobic spacer [Fig. 12(b)]. The corresponding distances $d1$ and $d2$ is ~3.384(3) Å and ~9.193(3) Å between the polar sheets.

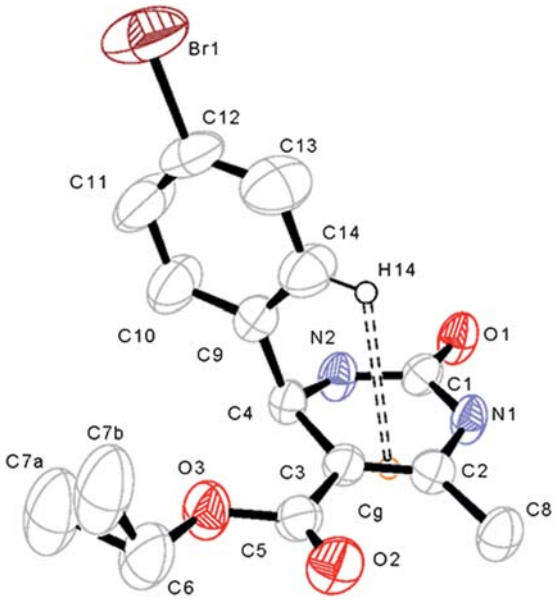

Fig. 11 ORTEP for **PYRO4** drawn at 50% ellipsoidal probability. Orange open circle Cg1 indicates the center of gravity of the double bond C2═C3 and the dotted line depicts C–H… π intra-molecular interaction. H atoms not involved in intra-molecular interactions are omitted for clarity.

Structure of PYRO5

The introduction of a methyl group in the *para* position on the phenyl ring [Fig. 13] results in the compound crystallizing in the monoclinic space group $P2_1/n$ with $Z = 8$ ($Z' = 2$) molecules in the unit cell, and is isostructural with **PYRO2B** and **PYRO3**. The dihedral angle between the tetrahydropyrimidine ring and the aryl moiety is 75.0(1)°/79.9(1)° in molecule A and B, respectively. Both the molecules exists in *s-cis* orientation with respect to the double bond. The crystal packing exhibits similarity in supramolecular features to **PYRO2B** and **PYRO3**. Strong N–H···O═C hydrogen bonded dimers (present in the asymmetric unit) generate a ribbon motif [Fig. 14(a)] These ribbons are further supported by C–H···O intermolecular interactions [Fig. 14(b)]. The space between two adjacent polar sheets is stabilized by van der Waals interactions [Fig. 14(b)]. The distance between the polar sheets *d*1 and *d*2 (sheets containing the non-polar aromatic moieties) are ~3.608(3) Å and ~9.867(3) Å, respectively.

Structure of PYRO6

The introduction of a methoxy moiety in the *para* position on the phenyl ring results in the compound [Fig. 15] crystallizing in monoclinic centrosymmetric space group $P2_1/n$ with $Z = 8$ ($Z' = 2$) in the unit cell. The molecule exists in the screw boat conformation. It is noteworthy that the primary crystal packing is governed by "similar" supramolecular motifs which dictate packing of molecules as observed in those of the previous compounds, namely **PYRO2B**, **3**, and **5**. The N–H···O═C hydrogen bonded dimers form a ribbon motif [Fig.16(a)] run along the crystallographic *b* axis further stabilized by C–H···O intermolecular interactions in the crystal lattice [Fig.16(b)]. The distance *d*1 between the "polar part" of the sheet like structure is ~3.696(3) Å and *d*2 is 10.521(4) Å (between molecule A and B in

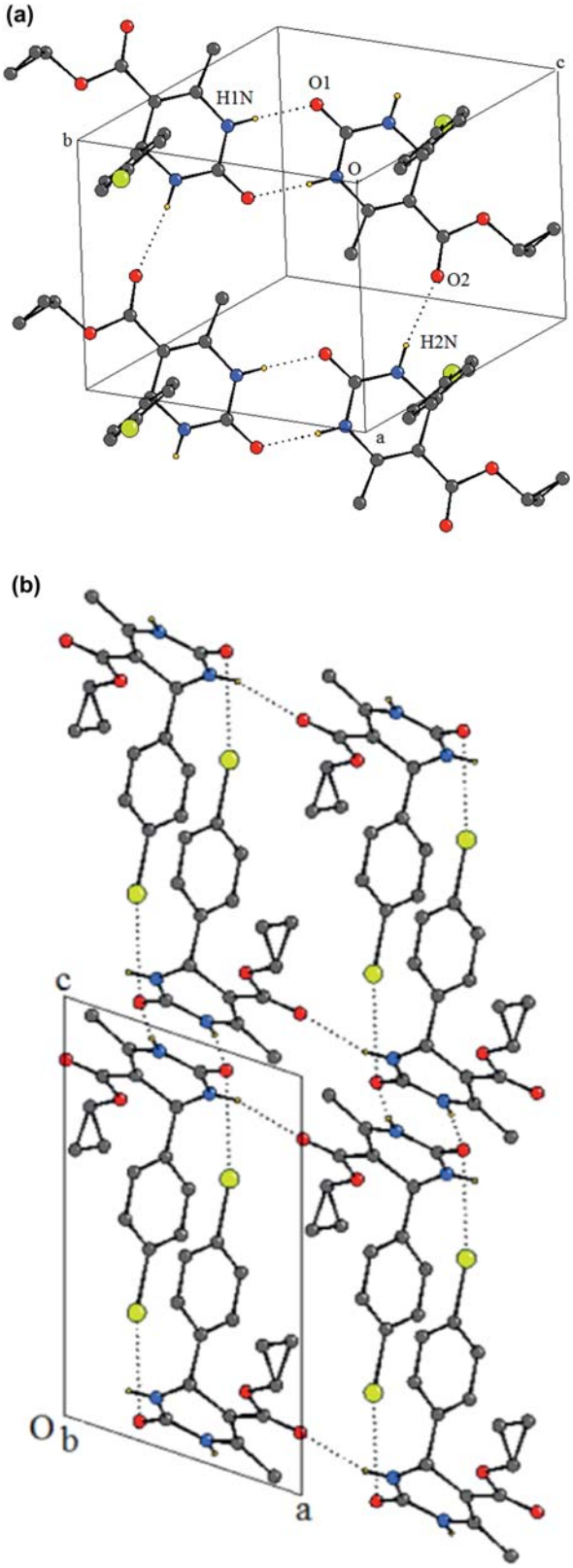

Fig. 12 (a) Packing motif in **PYRO4** depicting N–H···O hydrogen bonded dimers and chains along the crystallographic *a* axis. (b) Packing diagram in **PYRO4** depicting N–H···O hydrogen bonded dimers and chains along with C–Br···O═C dimeric short contacts in the crystal lattice. H atoms not involved in intermolecular interactions are omitted for clarity.

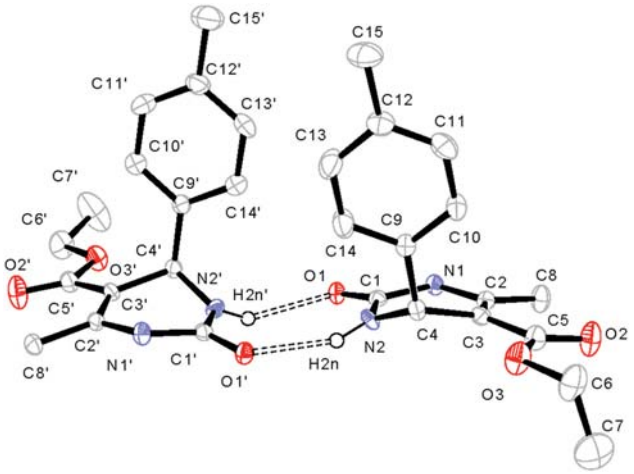

Fig. 13 ORTEP for **PYRO5** drawn at 50% ellipsoidal probability. Hydrogen atoms have been omitted for clarity.

the unit cell). The increase in distance *d*2 results from an increase in the steric requirements of the methoxy group in the *para* position.

Structure of PYRO7

On changing the position of the methoxy group from the *para* to the *meta* position on the phenyl ring [Fig. 17], the compound crystallizes in the monoclinic $P2_1/n$ space group with $Z = 4$ ($Z' = 1$) molecules in the unit cell. It is observed that the orientation of the ester moiety becomes *s-cis* with respect to the C2═C3 double bond. The crystal packing is dictated by dimeric motifs utilizing N–H···O═C intermolecular hydrogen bonds, involving H1N and H2N, forming a $R^2_2(8)$ ring motif generating ribbons [Fig. 18(a)] along the *b* axis. Furthermore, C–H···O interactions (involving H12) forming chains along the *b* axis and C–H···π interactions involving H7C, the terminal hydrogen of the C7 methyl group of the ester moiety, forming chains along the *n*

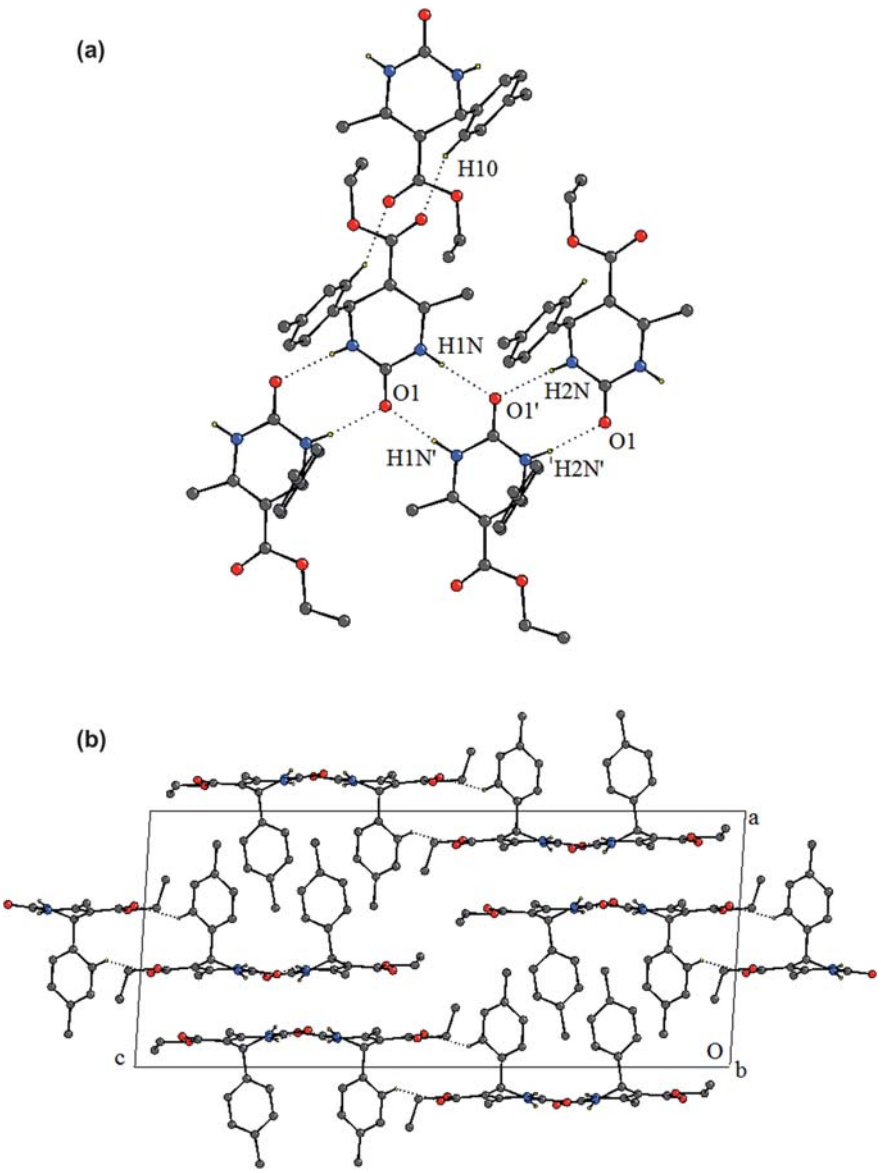

Fig. 14 (a) Formation of the ribbon motif utilizing N–H···O hydrogen bonds stabilized by C–H···O interactions in **PYRO5**. (b) Packing diagram of **PYRO5** depicting C–H···O intermolecular dimers. H atoms not involved in intermolecular interactions are omitted for clarity.

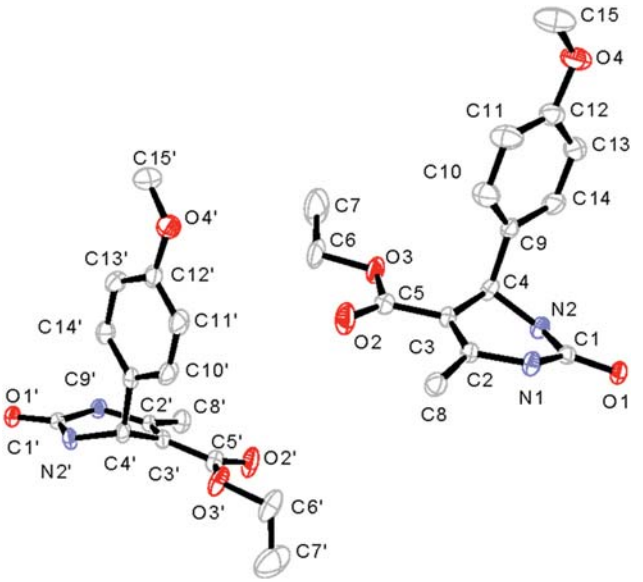

Fig. 15 ORTEP for **PYRO6** drawn at 50% ellipsoidal probability. Hydrogen atoms have been omitted for clarity.

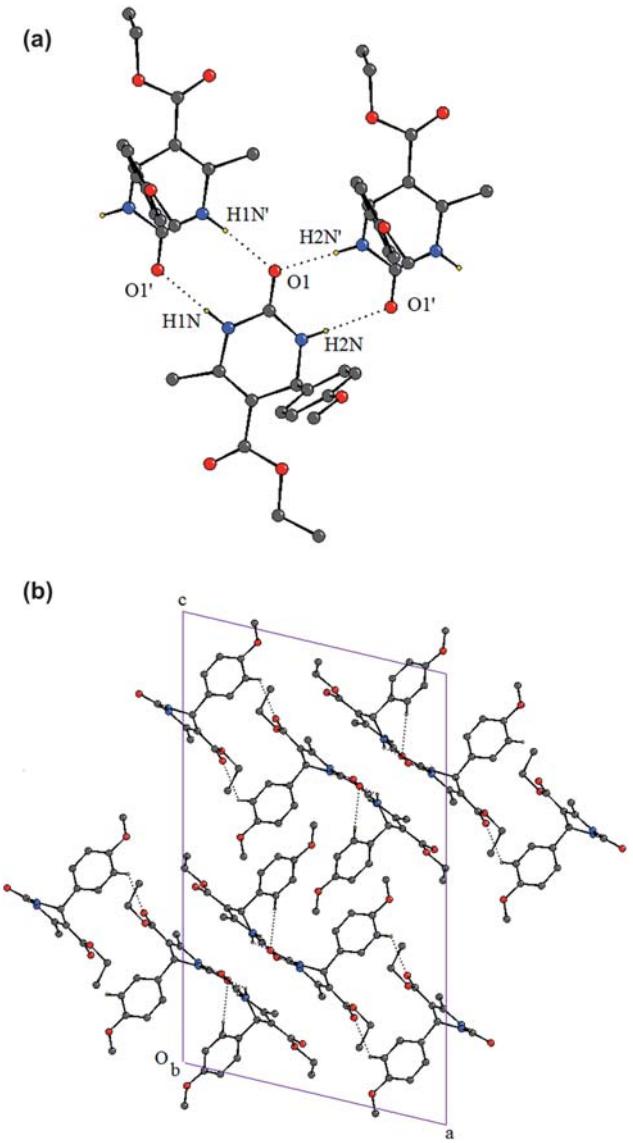

Fig. 16 (a) Formation of the ribbon motif utilizing N–H···O hydrogen bonds in **PYRO6**. (b) Packing diagram of **PYRO6** depicting C–H···O intermolecular interactions down the *ac* plane. H atoms not involved in intermolecular interactions are omitted for clarity.

glide plane, provide additional stability to the crystal packing [Fig. 18(b)]. The relevant distances *d*1 and *d*2 are ~3.453(3) Å and ~7.893(4) Å, respectively, in the crystal packing between the polar sheets and such sheets separated by the hydrophobic spacer.

Structure of PYRO8

This compound crystallizes in the monoclinic space group $P2_1/n$ space group with $Z = 4$ ($Z' = 1$) molecules in the unit cell [Fig. 19]. The presence of a methoxy substituent at the *meta* position and a hydroxy group at the *para* position results in a twist boat conformation for the six-membered tetrahydropyrimidine ring. The orientation of the ester moiety is *s-cis* with respect to the double bond. The carbon atom C6 (belonging to the ethyl moiety of the ester group) exhibits positional disorder, the occupancy of the major conformer refining to 0.76(2). The crystal packing is again controlled by N–H···O dimeric motifs forming a ribbon motif along the *b* axis [Fig. 20(a)]. The hydroxyl group participates in very weak O–H···O intermolecular hydrogen bonding. There are two different C–H···π intermolecular interactions stabilising the packing between the polar sheets, utilizing the screw axis and glide plane as the symmetry elements in the crystal lattice [Fig. 20(b)]. Thus the crystal packing is formed *via* a subtle interplay of strong and weak interactions.

Discussions and comparison with related structures (containing oxo moiety) in the CSD

A detailed crystallographic investigation of all the tetrahydropyrimidine derivatives containing multiple functional groups provides pointers towards an understanding of the key features in molecular recognition and relevant intermolecular contacts. These are responsible for the molecules to pre-organize and contribute towards the stability of the crystalline lattice. Due to the delocalization of the lone pair of electrons from either of the nitrogen atoms N1 and N2 over the C=O functional group the nitrogen atoms acquires considerable positive charge and the oxygen atoms acquire considerable negative charge.[21] Similar behaviour was observed in the sulfur containing analogs of these Bignelli compounds.[1] Here also the charge present on the sulfur atoms depends on the number of adjacent nitrogen atoms which by resonance with the C=S group leads to an increase in dipole moment. This results in an increased propensity to form N–H···S=C hydrogen bonds.[21]

The crystal structures discussed here can be categorized into two different supramolecular motifs, one constructed utilizing strong hydrogen bonds involving polar functional groups, and the other built up using hydrophobic moieties. The comparison of related crystal structures[22] in the Cambridge

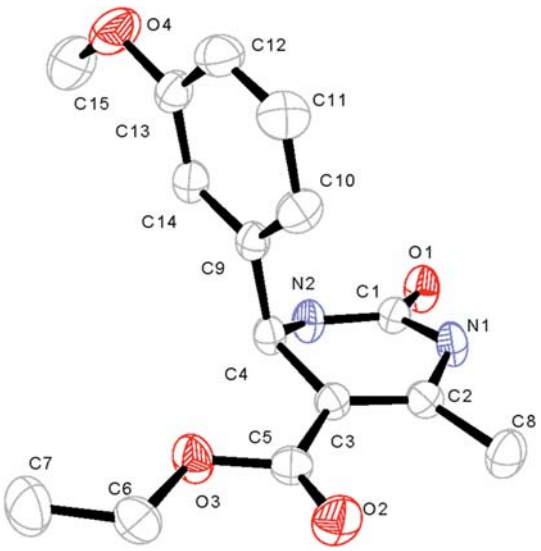

Fig. 17 ORTEP for **PYRO7** drawn at 50% ellipsoidal probability. The ester moiety exists in *s-cis* orientation with respect to the C2=C3 double bond. The hydrogen atoms have been excluded for clarity.

Structural Database (CSD) with the current compounds or interest is performed on the invariant molecular skeleton which has the ethyl-6-methyl-4-phenyl-2-oxo-1,2,3,4-tetrahydropyrimidine-5-carboxylate core.

The first member of comparison is the crystal structure of **YEYFOY**,[23] containing only a phenyl group. This compound also exists as a polymorph (**PIYYEC**).[24] The former crystallizes in $P2_1$ with $Z = 4$ ($Z' = 2$) and the latter in $P\bar{1}$ containing $Z' = 1$ molecule in the asymmetric unit. It is noteworthy that **PIYYEC** is also isostructural with **PYRO1** (CILSUM)[15] containing fluorine atom on the phenyl ring in the *ortho* position. The distances *d*1 and *d*2 are ~3.378(3) Å and ~7.549(4) Å in **PIYYEC** which are comparable with those in **PYRO1**. The crystal structure (**PIYYEC**) packs utilizing N–H···O=C hydrogen bonds forming dimers and chains generating a sheet-like structure. In contrast in the other polymorph *i.e.* **YEYFOY** containing two independent molecules in the asymmetric unit (closely related by a 2_1 screw axis), each molecule forms a ribbon motif utilizing N–H···O=C hydrogen bonds in the crystal lattice. Thus the two polymorphs are built up using two distinctly different structural motifs which direct packing of molecules. This is the only example of a Bignelli compound to exhibit dimorph formation, in addition to polymorph formation in **PYRO2**. Here also in **PYRO2B**, the two molecules in the asymmetric unit are closely related by an *n*-glide symmetry element. Another key structural feature is the alteration in the distance between two consecutive polar sheets, one where these directly face each other [*d*1] and the other where the hydrophobic moieties face each other [*d*2], each related by an inversion center due to the presence of various functionalities on the phenyl ring. The presence of a 3,4-methylenedioxophenyl moiety (**EXEPAY**)[25] results in the alteration of these distances, these being ~3.495(3) Å and ~9.339(4) Å, respectively. The substitution of a chloro group at the *ortho* position on the phenyl ring (**ILAHEI**),[26] results in isostructurality with **PYRO1** and **PIYYEC**, the corresponding distances are ~3.351(3) Å and ~7.771(4) Å, respectively. The space between the polar sheets in

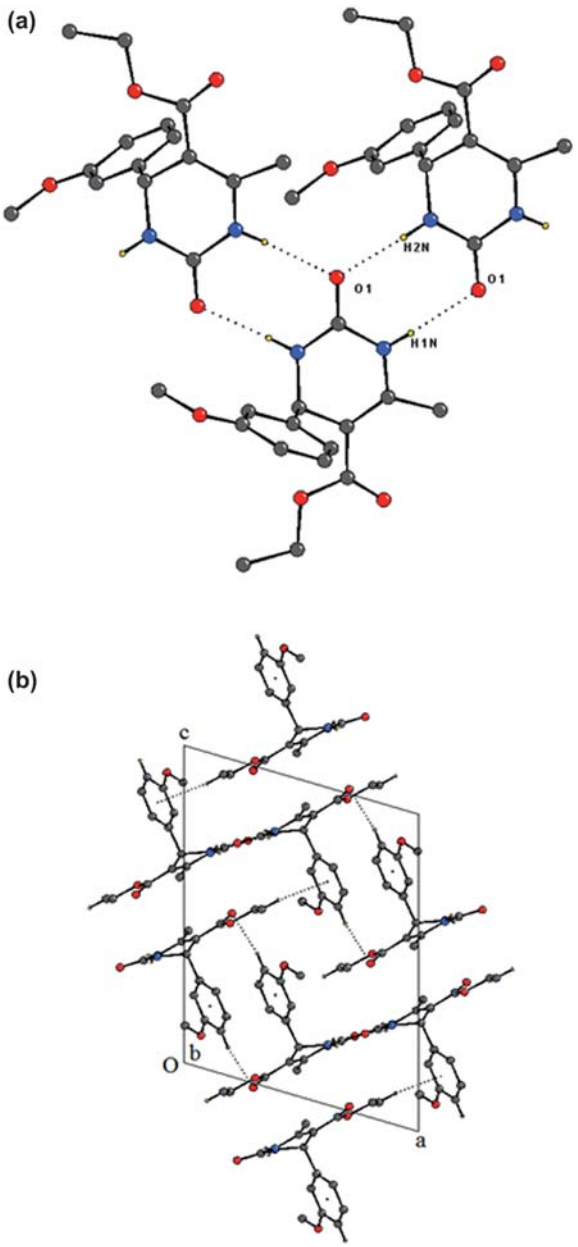

Fig. 18 (a) The ribbon motif formed using N–H···O intermolecular hydrogen bonds in **PYRO7**. (b) Packing diagram in the *ac* plane depicting C–H···O and C–H···π interactions. H atoms not involved in intermolecular interactions are omitted for clarity.

ILAHEI is stabilized by edge-to-edge and face-to-face aromatic stacking interactions between the chlorophenyl groups, the distances being ~3.537(3) Å and ~3.786(4) Å, respectively. Here again the crystal structure packs utilizing motifs similar to those observed in **PYRO1** and **PIYYEC**. The introduction of an electron-withdrawing nitro group (**REWDUS**)[27] results in a drastic change in the crystal packing features. The ester moiety has a different conformation (torsion being 125.1°), the role of sterics leads to the nitrophenyl group being rotated away from the methyl group of the ester moiety. One of the N–H donor forms N–H···O=C hydrogen bonds generating dimeric motifs. The other N–H donor also generates N–H···O hydrogen bond

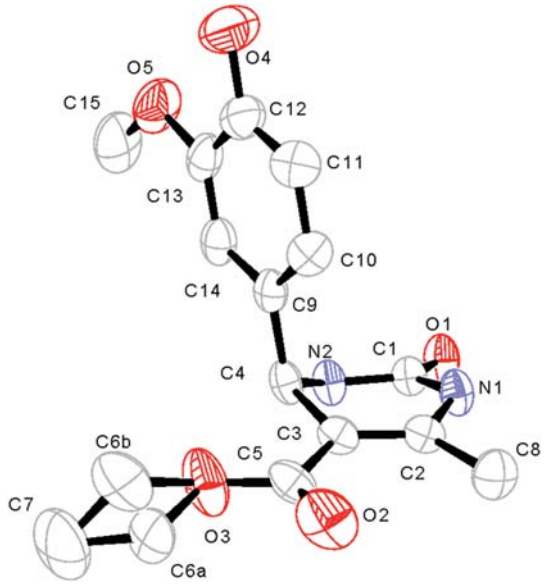

Fig. 19 ORTEP for **PYRO8** drawn at 50% ellipsoidal probability. The ester moiety exists in *s-cis* orientation with respect to the C2═C3 double bond. The hydrogen atoms have been excluded for clarity.

forming a discrete motif. Two such pairs hold two dimeric units (from both sides) together leading to the formation of an octameric unit (Fig. 21). These octameric motifs are further stabilized by intermolecular interactions between the electron deficient nitrophenyl ring and relatively electron rich tetrahydropyrimidine ring (the average distance between all the overlapping atoms of these two rings being ~3.735 Å). The two rings are further rotated with respect to each other forming a staggered conformation (Fig. 21). From a CSD study, it is noteworthy, that from reported crystal structures (in this class of compounds) in the literature, the crystal density observed for this particular *nitro* derivative [1.439 g cm^{-3}] is the highest.

The presence of a hydroxy group in the *ortho* position (**RICDAJ**)[28] generates O–H···O═C hydrogen bonds and hence disrupts the formation of "regular motifs (consisting of either dimers and chains forming sheets or a ribbon motif using N–H···O═C hydrogen bonds)" in the crystal lattice. A further comparison of these structures with **YAMQAF**[29] (hydroxyl group in *para* position of the phenyl ring) results in the formation of dimeric motif utilizing N–H···O═C hydrogen bonds, two such dimeric motifs being bridged by N–H···O–C(sp^2, aromatic) and O–H···O═C intermolecular hydrogen bonds involving the hydroxyl group generating a tetrameric motif (Fig. 22). Thus the crystal packing is different because of the participation of the hydroxyl group as a donor and an acceptor in molecular recognition.

Another notable structural feature in these class of compounds is the presence of disorder in the ethyl group of the ester moiety, a feature observed in **YAMQAF** also. This feature, which is apparently responsible for the C(sp^3–sp^3) bond shortening, has been investigated in detail by performing variable single crystal X-Ray diffraction on a crystal of racemic 1,1′-binaphthalene-2,2′-diyldiethylbis(carbonate) arising mainly due to positional disorder at two sites, with minor perturbations arising as a result of thermal vibrations.[30]

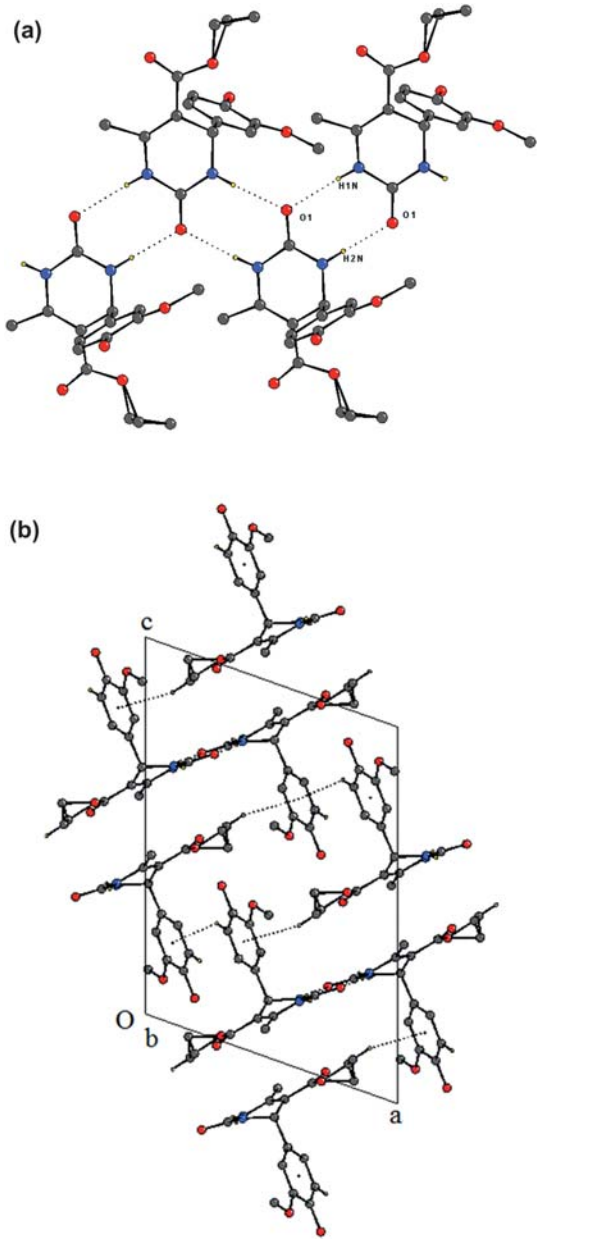

Fig. 20 (a) Formation of the ribbon motif utilizing N–H···O hydrogen bonds in **PYRO8**. (b) Packing diagram of **PYRO8** depicting N–H···O hydrogen bonded dimers perpendicular to *ac* plane, along with C–H···π intermolecular interactions. H atoms not involved in intermolecular interactions are omitted for clarity.

Such studies resolve the differences in molecular conformation at the ester group which is of significance in the context of conformational polymorphism.

Discussions and comparison with related structures (containing thioxo moiety)[1] in the CSD

It is also of interest to consider the similarities in molecular conformation and crystal packing of these compounds with those determined in the thioxo series.[1] It is noteworthy that **PIYYEC** is also isostructural with **PYR 1**(*para*-F), **3** (*meta*-Cl), **4** (*para*-methyl), **5** (*para*-*N*,*N*-dimethyl) compounds (in the thioxo

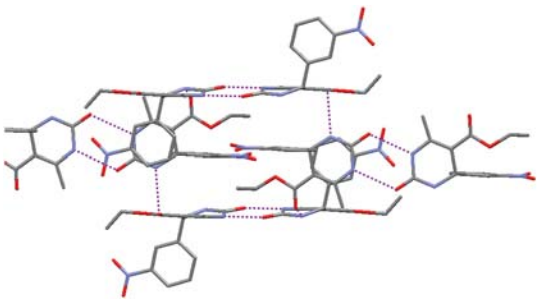

Fig. 21 Packing diagram in **REWDUS** depicting N–H···O=C hydrogen bonds generating an octameric unit. The two six-membered rings are in staggered conformation.

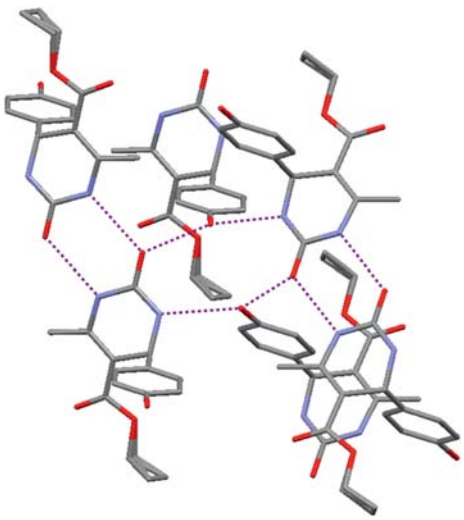

Fig. 22 Packing diagram in **YAMQAF** depicting N–H···O and O–H···O hydrogen bonds generating a tetrameric unit.

series). **ILAHEI** (*ortho* chloro in oxo series) is isostructural with **PYR1** (*para* F) in oxo series. The compound also exists in a screw boat conformation being stabilized by intra-molecular C–H···π interaction. **PYRO 7** (*meta*-methoxy) is isostructural with **PYR7** (*meta*-methoxy) from the thioxo series. The molecular conformation of these oxo compounds does not indicate the presence of intra-molecular C–H···π interaction (a significant feature observed in the corresponding thioxo series) indicating that the aryl ring is free to rotate with respect to the six-membered tetrahydopyrimidine ring.

Conclusions

In this article, we report the synthesis and characterization of eight differently substituted tetrahydropyrimidine derivatives (varying functional group substitution on the phenyl ring). The ester moiety exists in an *s-cis* orientation in all compounds. However the ethyl group of the ester moiety exists in different molecular orientations in differently substituted derivatives. In some cases, it also exhibits positional disorder, due to the greater thermal motion of the ethyl group. It is noteworthy that **PYRO2B**, **3**, **5** and **6** crystallizes with more than one molecule in the asymmetric unit. The existence of concomitant polymorphism in **PYRO2** points to the significance of positional disorder. It is the "freezing out" of these independent conformations whose signature is present in the asymmetric unit and hence gives rise to the presence of conformational polymorphism. The nucleating units contain this information and the molecular recognition events eventually giving rise to crystal formation. In all these crystal structures it is the formation of N–H···O hydrogen bonds giving rise to different structural motifs, namely dimers, chains and ribbon motifs along with the presence of weak C–H···O and van der Waals interactions which contribute towards the overall crystal packing.

Acknowledgements

Susanta K. Nayak thanks CSIR for research fellowship. We all thank IISc, Bangalore X-ray facility under the DST, India scheme. The authors also thank Mr. M. R. Vippila for recording all the ^{1}H-NMR of the compounds under study.

Notes and references

1 S. K. Nayak, K. N. Venugopala, D. Chopra, Vasu and T. N. Guru Row, *CrystEngComm*, 2010, **12**, 1205–1216.
2 C. O. Kappe, W. M. F. Fabian and M. A. Semones, *Tetrahedron*, 1997, **53**, 2803–2816.
3 O. V. Shishkin, E. V. Solomovich, V. M. Vakula and F. G. Yaremenko, *Russ. Chem. Bull.*, 1997, **46**, 1941–1946.
4 K. Devi, K. N. Venugopala, G. K. Rao and P. N. S. Pai, *InPharm Communique.*, 2008, **1**, 19–24.
5 *SMART (V 5.628), SAINT (V 6.45a), Sadbs, XPREP, SHELXTL*; Bruker AXS Inc.; Madison, WI, 2004.
6 Oxford Diffraction (2009). *CrystAlis CCD and CrystAlis RED*, Version 1.171.33.31. Oxford Difraction Ltd. Abingdon, Oxfordshire, England.
7 G. M. Sheldrick, *Acta Crystallogr., Sect. A: Found. Crystallogr.*, 2008, **64**, 112–122.
8 L. J. Farrugia, WinGX (V 1.70.01, *J. Appl. Crystallogr.*, 1999, **32**, 837.
9 L. J. Farrugia, *J. Appl. Crystallogr.*, 1997, **30**, 565.
10 C. F. Macrae, I. J. Bruno, J. A. Chisholm, P. R. Edgington, P. McCabe, E. Pidcock, L. Rodriguez-Monge, R. Taylor, J. van de Streek and P. A. Wood, *J. Appl. Cryst.*, 2008, **466**, 41, http://www.ccdc.cam.ac.uk/mercury.
11 M. J. Nardelli, *J. Appl. Crystallogr.*, 1995, **28**, 659.
12 A. L. Spek, *Acta Crystallogr., Sect. D: Biol. Crystallogr.*, 2009, **65**, 148–155.
13 M. J. Frisch, G. W. Trucks, H. B. Schlegel, G. E. Scuseria, M. A. Robb, J. R. Cheeseman, J. A. Jr. Montgomery, T. Vreven, K. N. Kudin, J. C. Burant, J. M. Millam, S. S. Iyengar, J. Tomasi, V. Barone, B. Mennucci, M. Cossi, G. Scalmani, N. Rega, G. A. Petersson, H. Nakatsuji, M. Hada, M. Ehara, K. Toyota, R. Fukuda, J. Hasegawa, M. Ishida, T. Nakajima, Y. Honda, O. Kitao, H. Nakai, M. Klene, X. Li, J. E. Knox, H. P. Hratchian, J. B. Cross, V. Bakken, C. Adamo, J. Jaramillo, R. Gomperts, R. E. Stratmann, O. Yazyev, A. J. Austin, R. Cammi, C. Pomelli, J. W. Ochterski, P. Y. Ayala, K. Morokuma, G. A. Voth, P. Salvador, J. J. Dannenberg, V. G. Zakrzewski, S. Dapprich, A. D. Daniels, M. C. Strain, O. Farkas, D. K. Malick, A. D. Rabuck, K. Raghavachari, J. B. Foresman, J. V. Ortiz, Q. Cui, A. G. Baboul, S. Clifford, J. Cioslowski, B. B. Stefanov, G. Liu, A. Liashenko, P. Piskorz, I. Komaromi, R. L. Martin, D. J. Fox, T. Keith, M. A. Al-Laham, C. Y. Peng, A. Nanayakkara, M. Challacombe, P. M. W. Gill, B. Johnson, W. Chen, W. M. Wong, C. Gonzalez, J. A. Pople, *Gaussian 03*, revision B.03; Gaussian, Inc.: Wallingford, CT, 2004.
14 D. Cremer and J. A. Pople, *J. Am. Chem. Soc.*, 1975, **97**, 1354–1358.
15 L. Ming, G. W. Si, W. L. Rong, L. Y. Feng and Y. H. Zheng, *J. Mol. Catal. A: Chem.*, 2006, **258**, 133–138.
16 (*a*) D. Chopra and T. N. Guru Row, *Cryst. Growth Des.*, 2006, **6**, 1267–1270; (*b*) D. Chopra, V. Thiruvenkatam and T. N. Guru

Row, *Cryst. Growth Des.*, 2006, **6**, 843–845; (*c*) D. Chopra and T. N. Guru Row, *Cryst. Growth Des.*, 2008, **8**, 848–853.
17 J. Bernstein, R. Davis, E. L. Shimoni and N.-L. Chang, *Angew. Chem., Int. Ed. Engl.*, 1995, **34**, 1555–1573.
18 (*a*) D. Chopra and T. N. Guru Row, *Cryst. Growth Des.*, 2005, **5**, 1679–1681; (*b*) D. Chopra and T. N. Guru Row, *CrystEngComm*, 2008, **10**, 54–67; (*c*) D. Chopra, T. S. Cameron, J. D. Ferrera and T. N. Guru Row, *J. Phys. Chem. A*, 2006, **110**, 10465–10477; (*d*) D. Chopra, V. Thiruvenkatam, S. G. Manjunath and T. N. Guru Row, *Cryst. Growth Des.*, 2007, **7**, 868–874.
19 (*a*) V. R. Thalladi, H.-C. Weiss, D. Bläser, R. Boese, A. Nangia and G. R. Desiraju, *J. Am. Chem. Soc.*, 1998, **120**, 8702–8710; (*b*) Deepak Chopra, K. Nagarajan and T. N. Guru Row, *J. Mol. Struct.*, 2008, **888**, 70–83.
20 M. Nishio, Y. Umezawa, K. Honda, S. Tsuboyama and H. Suezawa, *CrystEngComm*, 2009, **11**, 1757–1788.
21 P. A. Wood, E. Pidcock and F. H. Allen, *Acta Crystallogr., Sect. B: Struct. Sci.*, 2008, **64**, 491–496.
22 Cambridge Structural Database Version 5.30, November 2008. A molecular search in the CSD analysis resulted in 11 unique hits. The crystal structures selected have 3D coordinates and R-Factor below 0.10. The REF codes obtained are **CILSUM**, **EXEPAY**, **IBESAK**, **ILAHEI**, **LOCCOW**, **REWDUS**, **RICDAJ**, **XECHUJ**, **YAMQAF**, **YEYFOY**, and **PIYYEC** (polymorph of **YEYFOY**), respectively. All these structures were analyzed using the software Mercury[10] for comparison with our structures and identify the differences in molecular geometry, conformation and packing features associated with these compounds.
23 **YEYFOY**:Q.-F. Cheng, X.-Y. Xu, P.-F. Shi and X.-L. Hu, *Acta Crystallogr., Sect. E: Struct. Rep. Online*, 2007, **63**, o468.
24 **PIYYEC**:M. N. Mohideen, A. Rasheeth, C. A. M. A. Huq and S. S. Nizar, *Acta Crystallogr., Sect. E: Struct. Rep. Online*, 2008, **64**, o1752.
25 **EXEPAY**:S.-J. Tu, F. Fang, H. Jiang, S.-L. Zhu, T.-J. Li, X.-J. Zhang and D.-Q. Shi, *Chin. J. Struct. Chem.*, 2004, **23**, 494.
26 **ILAHEI**:S.-J. Tu, F. Fang, Y. Gao, H. Jiang, C.-B. Miao and D.-Q. Shi, *Chin. J. Struct. Chem.*, 2003, **22**, 617.
27 **REWDUS**:G. C. Rovnyak, S. D. Kimball, B. Beyer, G. Cucinotta, J. D. Di Marco, J. Gougoutas, A. Hedberg, M. Malley, J. P. McCarthy, R. Zhang and S. Moreland, *J. Med. Chem.*, 1995, **38**, 119.
28 **RICDAJ**:Q.-F. Cheng, X.-Y. Xu, J.-Y. Bao and C.-F. Zhang, *Acta Crystallogr., Sect. E: Struct. Rep. Online*, 2007, **63**, o2391.
29 **YAMQAF**:M. Li, W.-S. Guo, L.-R. Wen and W.-Y. Qi, *Acta Crystallogr., Sect. E: Struct. Rep. Online*, 2005, **61**, 531.
30 S. K. Nayak, S. Chandrasekhar and T. N. Guru Row, *Acta Crystallogr., Sect. C: Cryst. Struct. Commun.*, 2009, **65**, o222–o225.